Total Environment Engineering 6 (2026) 100070

Contents lists available at ScienceDirect

Total Environment Engineering

journal homepage: www.elsevier.com/locate/teengi

Role and mechanism of rare earth oxides in alleviating ammonia inhibition and facilitating methanogenesis

Ting-ting Yang [a], Zhi-Man Yang [a,*], Zhi-Biao Chen [b], Zu-Liang Chen [a]

[a] Fujian Key Laboratory of Pollution control & Resource Reuse, College of Environmental and Resource Sciences, Fujian Normal University, Fuzhou, China
[b] Key Laboratory for Humid Subtropical Eco-Geographical Processes of the Ministry of Education, School of Geographical Sciences, Fujian Normal University, Fuzhou, China

ARTICLE INFO

Keywords:
Anaerobic digestion
Methane
Ammonia inhibition
Rare earth oxides
Direct interspecies electron transfer

ABSTRACT

Rare earth oxides (REOs) have been shown to effectively promote methane production, yet little is known about their role in the anaerobic digestion (AD) process under ammonia stress. The aim of this work was to investigate the influence of REOs on methane production under ammonia stress. Lanthanum oxide (LO), yttrium oxide (YO) and neodymium oxide (NO) were prepared via direct pyrolysis at 800 °C, and their roles in AD were systematically investigated. Compared to NO, LO and YO exhibited a higher electron exchange capacity (EEC), indicating their superior performance in facilitating electron transfer during AD. LO performed better than YO and NO in promoting methanogenesis, resulting in a 26% increase in methane yield and a 24 % increase in the maximum methane production rate compared to the control group. Microbial analysis showed that REOs facilitated the enrichment of putative electroactive *Trichococcus* and *Methanosarcina*. Apart from potentially promoting the putative direct interspecies electron transfer (DIET) between these two microbes, LO could also boost methanogenesis, potentially by enhancing alternative pathways such as acetate decarboxylation and utilization of H_2, methanol, and methylamine. However, YO and NO promoted methane yield likely by facilitating the acetate decarboxylation and the utilization of H_2, methanol, and methylamine, whereas the putative DIET pathway played only a minor role. This work offers some important references for the operation of laboratory-scale and batch AD systems subjected to high ammonia stress.

1. Introduction

Anaerobic digestion (AD) has been extensively employed for treating diverse biomass wastes while concurrently generating renewable energy in the form of methane (CH_4) (Xu et al., 2022). *Dicranopteris pedata* has been widely used in ecological restoration in rare earth mining areas, and its biomass is rich in cellulose, hemicellulose, and lignin (Feng et al., 2025). AD of *Dicranopteris pedata* biomass (DPB) can not only facilitate the resource utilization but also provide a viable pathway for renewable energy supply. However, during the AD process, the accumulation of ammonia nitrogen (NH_4^+-N) is recognized as a critical inhibitor of methanogenesis, with reported inhibitory thresholds ranging from 1.7 to 14 g/L (Chen et al., 2008; Shapovalov et al., 2020). High NH_4^+-N concentrations can severely inhibit methanogenesis, not only reducing CH_4 yield by over 30 % but potentially causing complete system collapse and termination of all methanogenic activity (Cai et al., 2021b; Ngo et al., 2022, 2023). Ammonia nitrogen exists in two forms: ammonia ions (NH_4^+) and free ammonia (NH_3, FAN), both of which can directly or indirectly inhibit the anaerobic digestion process (Mlinar et al., 2022). Hydrophobic NH_3 molecules enter microbial cells via passive diffusion, where they combine with intracellular protons (H^+) to form NH_4^+ (Shi et al., 2017). This process not only consumes protons essential for maintaining energy metabolism but also alters intracellular pH, thereby disrupting the transmembrane proton gradient and ATP synthesis. High NH_4^+-N can also alter microbial community structure and function, leading to excessive accumulation of certain volatile fatty acids (VFAs). Propionate, in particular, is more susceptible to NH_4^+-N effects, which can hinder its degradation and lead to reduced CH_4 production (Bonk et al., 2018; Guo et al., 2024; Yang et al., 2024). Novel methods and strategies are urgently needed to address ammonia inhibition in AD.

The fundamental principle of direct interspecies electron transfer (DIET) involves the electron exchange between VFA-oxidizing bacteria and electron-accepting methanogens. Unlike traditional pathways that involved the release of soluble electron carriers such as hydrogen (H_2) or

* Corresponding author.
E-mail address: yangzm@fjnu.edu.cn (Z.-M. Yang).

https://doi.org/10.1016/j.teengi.2026.100070
Received 18 November 2025; Received in revised form 30 January 2026; Accepted 14 February 2026
Available online 14 February 2026

formate, the released electrons by VFA-oxidizing bacteria are directly transferred to adjacent methanogens (Al Hasani et al., 2025). The mechanism of DIET primarily involves electron transfer through conductive components, such as cell surface cytochrome c, conductive pili, or externally introduced conductive materials (Al Hasani et al., 2025; Baek et al., 2018). Both carbon-based and iron-based conductive materials had been extensively used to enhance methane production in AD systems (Yin et al., 2020). These materials not only acted as electron carriers but also improved electron transfer efficiency by interacting with cytochrome c, pili, flavin, and the other components. Such mechanisms represented promising technical strategies for mitigating ammonia inhibition during AD (Baek et al., 2018; Lu et al., 2022). Table S1 lists the effectiveness of different conductive materials in boosting methane yield under high ammonia stress. For example, Wang and coworkers demonstrated that under an ammonia concentration of 6 g/L, biochar increased cumulative methane production by approximately 21 % and elevated the maximum methanogenic rate by 2.1-fold. This enhancement was attributed to the enrichment of putatively electroactive bacteria (e.g., *Clostridium*) and methanogens (e.g., *Methanosarcina*) and the subsequent establishment of DIET between them (Wang et al., 2023a). Similarly, Lu et al. reported that the addition of nano-Fe_3O_4 biochar under 5 g/L ammonia stress enhanced methane yield by 62.61 %, concomitant with the enrichment of potentially electroactive *Chloroflexi* and methanogenic *Methanosarcina*, thereby facilitating the DIET-mediated methanogenesis under high ammonia conditions (Lu et al., 2022). In addition, Dai et al. observed that the Fe_3O_4 addition enriched *Desulfobacterium, Clostridiales*, and *Methanothrix*, and increased methane yield by 13.8 % at 3 g/L of ammonia (Dai et al., 2024). Macrotranscriptomic analysis revealed that the Fe_3O_4 addition up-regulated conductive pili and cytochrome-related gene expression, indicating the key role of the Fe_3O_4-driven DIET-dependent methanogenesis (Dai et al., 2024).

Rare earth elements (REEs) have attracted growing interest due to their unique 4f electron configurations and redox couples (e.g., REE^{3+}/REE^{2+} or REE^{4+}/REE^{3+}), which confer potential application to AD (Liu et al., 2022; Rotaru et al., 2014; Su et al., 2024). Liu et al. demonstrated that supplementing wheat straw AD systems with low concentrations of cerium dioxide nanoparticles not only enriched *Methanobacterium* and *Methanosaeta* but also resulted in a 20.15 % increase in methane production (Liu et al., 2022). Similarly, Su et al. reported that La_2O_3 and CeO_2 could function as electron conduits to potentially facilitate DIET between Geobacter and Methanospirillum, thereby enhancing methane yield (Su et al., 2024). While it has been established that REOs can improve methane production in AD, the mechanisms underlying their potential to alleviate ammonia-induced inhibition remain unclear. To date, little is also known about the interplay among the AD performance, the electrochemical properties of REOs, and the functional microbial communities. Therefore, a comprehensive investigation is warranted to elucidate the fundamental mechanisms of ammonia inhibition and the mitigating effects conferred by REOs in AD systems.

In this study, three types of rare earth oxides (LO, YO, and NO) were synthesized through pyrolysis of their corresponding nitrates at 800 °C and subsequently introduced into AD systems to evaluate their distinct effects on mitigating ammonia inhibition. The research aimed to: (1) determine whether REOs could alleviate ammonia inhibition and promote methane production, and (2) investigate the mechanism by which REOs enhance CH_4 production. This work offers a novel approach to addressing ammonia inhibition during the AD process.

2. Methods and materials

2.1. DPB and inoculum

DPB collected from ion-type rare earth mining areas in Fujian Province was used as the raw material. The DPB samples were pulverized, dried, and screened. Samples with a particle size below 120 mesh were selected for AD, and their total solids (TS) and volatile solids (VS) were 91.05±0.08 % and 92.81±0.18 %, respectively. Anaerobic digestion sludge obtained from a laboratory reactor operating at 35 °C was used as inoculum to initiate methane production. The reactor was periodically fed with a mixture of *Pennisetum giganteum* biomass and kitchen waste at a mass ratio of 1:1. TS and VS of sludge were 10.46 ± 0.13 % and 58.09 ± 0.66 %, respectively.

2.2. Preparation of rare earth oxides

REOs were prepared in a tube furnace. $La(NO_3)_3{\cdot}6H_2O$, $Y(NO_3)_3{\cdot}6H_2O$, and $Nd(NO_3)_3{\cdot}6H_2O$ were separately placed in the tube furnace for calcination. Under an N_2 atmosphere, the furnace was first purged for half an hour, then heated at a rate of 5 °C/min with an N_2 flow rate of 250 ml/min to 800 °C. The temperature was maintained at the target value for 2 h. The resulting lanthanum oxide, yttrium oxide, and neodymium oxide were respectively ground into fine particles and stored in centrifuge tubes, which were labeled as LO, YO, and NO, respectively.

2.3. Anaerobic digestion experiment

This study was conducted in 120 mL anaerobic bottles with a working volume of 50 mL and an NH_4^+-N concentration of 5 g/L, under static incubation at 35 °C. The anaerobic digestion procedure was as follows: DPB (27.9 g-VS/L), individual REO (15 g/L), and sludge (8.7 g-VS/L) were introduced into the anaerobic bottles, followed by the addition of phosphate buffer solution and thorough mixing to initiate batch anaerobic digestion. Afterwards, to establish anaerobic environment, the bottles were sealed with butyl rubber stoppers and aluminum crimp caps, and their headspace air was replaced with high-purity N_2. Subsequently, 0.3 mL of 0.2 M sodium sulfide solution was injected to remove the residual dissolved O_2 in the culture medium. All experiments were performed in triplicate. The bottles supplemented with lanthanum oxide, yttrium oxide and neodymium oxide were designated as the LO, YO, and NO groups, respectively. The REO-unamended bottle was designated as the control group.

2.4. Analytical methods

X-ray diffraction (XRD) (Panalytical, model X'Pert Pro, Holland) was employed to identify the crystalline structure and phase composition of REOs (Tripathi et al., 2024). TS and VS were determined at 105 °C and 550 °C, respectively (Li et al., 2022). A three-electrode electrochemical cell was utilized to assess the electron accepting capacity (EAC), electron donating capacity (EDC), and electron exchange capacity (EEC) of REOs (Xu et al., 2025). The activity of the electron transfer system (ETS) was analyzed via the 2-(p-iodophenyl)-3-(p-nitrophenyl)-5-phenyl tetrazolium chloride (INT-ETS) assay (Shi et al., 2024). Cyclic voltammetry (CV) and differential pulse voltammetry (DPV) experiments were conducted using a 20 mL three-electrode electrochemical cell (Xu et al., 2025; Yang et al., 2022). Methane content was quantified by a gas chromatography (GC-2014C, Shimadzu, Japan), and volatile fatty acid (VFA) concentrations were detected by a gas chromatography equipped with a flame ionization detector (Xu et al., 2024, 2025). Methane production data were subjected to analysis of variance (ANOVA) using IBM SPSS 19.0.

At the end of AD, 7 g samples were collected and preserved at −80 °C. Amplicon sequencing of the extracted total genomic DNA was performed by Majorbio Inc. (Shanghai, China). Amplicon sequence variants (ASVs) were clustered and taxonomically classified using QIIME2. Based on the generated ASVs and the KEGG database, Phylogenetic Investigation of Communities by Reconstruction of Unobserved States 2 (PICRUSt2) was employed to predict functional genes associated with microbial metabolic pathways (Liu et al., 2025; Xu et al., 2025). Visualization of analysis results was performed using R version 4.3.3.

3. Results and discussion

3.1. Characterization of REOs

As shown in Fig. S1, the XRD patterns of the REOs showed distinct, sharp peaks matching the reference patterns for La_2O_3 (PDF#05–0602), Y_2O_3 (PDF#73–1334), and Nd_2O_3 (PDF#41–1089) (Alhassan et al., 2024; Chen et al., 2017; Kaya and Gürmen, 2020; Michel et al., 2013; Mu and Wang, 2011). The typical peaks for $La(OH)_3$ (PDF#06–0585) and $Nd(OH)_3$ (PDF#06–0601) were also observed in LO and NO, possibly due to the surface reaction of La_2O_3 and Nd_2O_3 with ambient water vapor (Luo et al., 2024). In addition, previous studies have demonstrated that EAC, EDC and EEC are key parameters for assessing the electron transfer capacity of conductive materials (Cruz et al., 2017). As shown in Table 1, compared to YO and NO, EAC of LO increased by 71.4 % and 54.3 %, respectively. Additionally, in comparison to LO and NO, EDC of YO increased by 62.3 % and 60.2 %, respectively. Notably, LO and YO had higher EEC values, which were 14.7 % and 38.4 % higher than that of NO, respectively. Thus, it was possible that LO and YO performed better than NO in facilitating electron transfer during AD (Qin et al., 2020).

3.2. AD performance

Methane production changes in the presence of REOs were shown in Fig. 1a. After ten days of AD, methane yields in the LO and YO groups were higher than that of the control group at each day point. However, after 35 days of AD, methane yield in the NO group exceeded that of the control group. Furthermore, the final methane yields of the LO, YO, and NO groups were 31.16, 30.45 and 29.87 mL/g-VS, representing increases of 26 %, 24 %, and 21 % over the control group, respectively (Table S2). These results indicated that LO, YO, and NO were beneficial for enhancing methane production and alleviating ammonia inhibition. In addition, under high ammonia stress, the methane yield in the REO-unamended group (24 mL/g-VS) was markedly lower than that in the non-ammonia inhibition group (67.29 ± 10.97mL/g-VS) (Fig. S2). This yield was also substantially lower than the value (85.36 mL/g-VS) reported in a prior study conducted without exogenous ammonia addition (Xu et al., 2025). This might be due to the fact that high ammonia concentrations severely inhibited the methanogenic activity (Shapovalov et al., 2020).

Kinetic analysis revealed that the addition of both LO and YO significantly enhanced the maximum methane production rate (Rm) (Table S2). Specifically, both LO and YO differentially enhanced Rm compared to the control group, with increases of 24 % and 17 %, respectively. However, the NO group exhibited a slight decrease in Rm relative to the control. Furthermore, LO, YO, and NO also shortened the lag-phase time. YO performed better than YO and NO in reducing the lag-phase time. The findings indicated that YO can effectively stimulate methane production at the early stage of AD compared to LO and NO.

As depicted in Fig. 1b, during the initial phase of anaerobic AD, all groups exhibited a sharp decrease in pH, likely attributable to the rapid accumulation of total VFAs. Compared to the control, the LO, YO, and NO groups exhibited a less pronounced decline in pH. After 15 days of AD, the LO, YO, and NO groups showed a rapid restoration in pH compared to the control group. However, the pH in the control group varied between 5.9 and 6.2 after 15 days of AD. These findings indicated that REOs could enhance the buffering capacity of the AD system.

Table 1
Electrochemical properties of REOs.

Material	EDC (mmol e^-/g)	EAC (mmol e^-/g)	EEC (mmol e^-/g)
LO	0.108±0.019	0.159±0.018	0.266±0.035
YO	0.063±0.007	0.258±0.039	0.321±0.039
NO	0.070±0.022	0.161±0.001	0.232±0.022

As illustrated in Fig. 2, VFAs were composed of acetate, propionate, butyrate, valerate, and caproate, with acetate and propionate identified as the predominant metabolites. All experimental groups exhibited a consistent pattern of initial VFA accumulation followed by subsequent degradation. The YO group reached peak concentration on day 5, whereas the LO and NO groups peaked on day 15. Moreover, substantial accumulation of propionate was observed across all groups. However, the REO-amended groups showed a rapid acetate consumption, with nearly complete acetate degradation at the end of AD. These results indicated that LO, YO, and NO were beneficial for the degradation of acetate rather than propionate under ammonia inhibition. The low propionate degradation may be attributed to a significant inhibition of the propionate-oxidating bacteria (e.g., *Syntrophobacter*) and disruption of syntrophic cooperation between the syntrophic bacteria and methanogens (Bonk et al., 2018; Guo et al., 2024; Lee et al., 2019; Yang et al., 2024).

3.3. Electrochemical analysis

CV scan showed that a pair of redox peaks was observed for each group (Fig. S3a). The peak intensity and integral area of CV curve were reported to be related to the electron exchange capacity of the AD systems (Liu et al., 2025). Compared to the control group, the LO and NO groups had a higher peak intensity and integral area, indicating an improvement of the electron exchange capacity of the AD systems. However, in comparison to the control group, YO did not cause an enhancement in the peak intensity and integral area, while it promoted methane production. This indicated that the electron exchange capacity of the YO-amended AD system made a minor contribution to the improved methanogenesis. It was possible that methane production from intermediates such as H_2, methanol or methylamine could also be stimulated during the AD of DPB (Liu et al., 2018; Xiao et al., 2019).

As shown in Fig. S3b, DPV scan showed that a typical peak at around 0 V was observed in all groups, which might be linked with the outer membrane c-type cytochromes (Okamoto et al., 2013; Wang et al., 2023b). Compared to the control group, YO and NO caused increases in the peak intensities, whereas LO showed a negative effect. The outer membrane c-type cytochromes were reported to participate in DIET (Zhao et al., 2020), suggesting its minor role in the LO-driven methanogenesis (Wang et al., 2021). Furthermore, Fig. 3 shows that the ETS activities in the LO, YO, and NO groups increased by 21 %, 32 %, and 24 % compared to the control group, respectively. It has been reported that microbial intracellular electron transfer (IET) capacity was related to the ETS activity (Zhuo et al., 2025), suggesting that LO, YO, and NO had the potential for enhancing the IET capability of microbes.

3.4. Microbial community analysis

The dominant bacterial genera were *Trichococcus, Clostridium, Brooklawnia, Proteiniphilum, Terrisporobacter, Thermovirga*, and *Bacteroides* (Fig. 4a). *Clostridium, Brooklawnia, Terrisporobacter*, and *Proteiniphilum* were reported to convert proteins, carbohydrates, and cellulose into VFAs (Cai et al., 2021a; Li et al., 2023b; Wu et al., 2021; Xiao et al., 2024; Yan et al., 2020). In addition, *Bacteroides* can convert carbohydrate to VFAs, H_2, and CO_2 for subsequent methanogenesis (Zhang et al., 2022). These bacterial genera were selectively enriched in the presence of LO, YO, and NO Specifically, compared to the control, the relative abundances of *Trichococcus* and *Proteiniphilum* increased on average by 2.8-fold and 1.3-fold in the LO, YO, and NO groups, respectively. Conversely, the relative abundances of *Clostridium* and *Terrisporobacter* decreased on average by 29 % and 38 %, respectively. Moreover, the relative abundances of *Bacteroides* decreased by 91 % and 80 % in the YO and NO groups, respectively, while LO showed a positive effect. In AD systems, high ammonia concentrations not only alter bacterial community structure but also inhibit acidogenesis, leading to substantial accumulation of VFAs (e.g., propionate) (Yang et al., 2024). In this work,

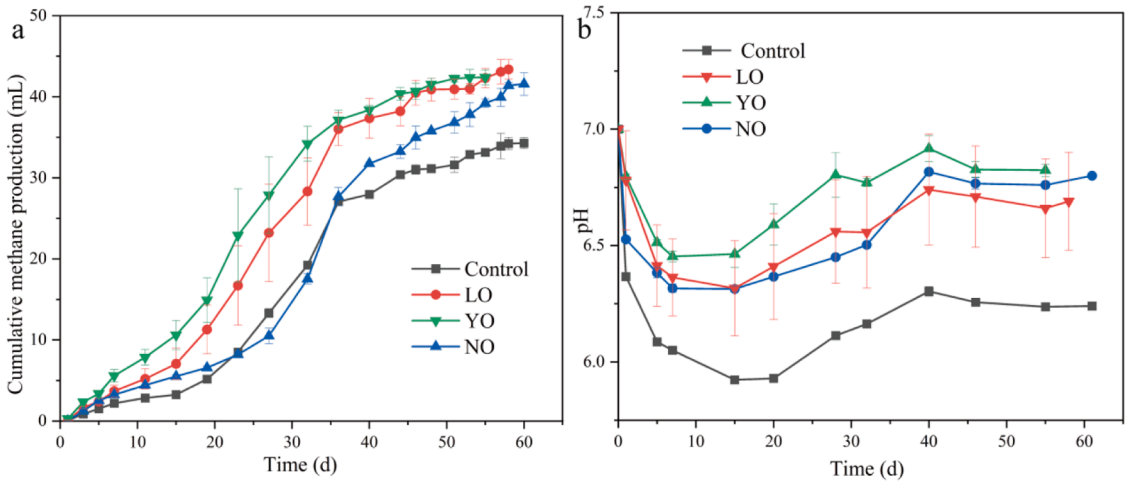

Fig. 1. Changes of cumulative methane production (a) and pH (b) during the AD process.

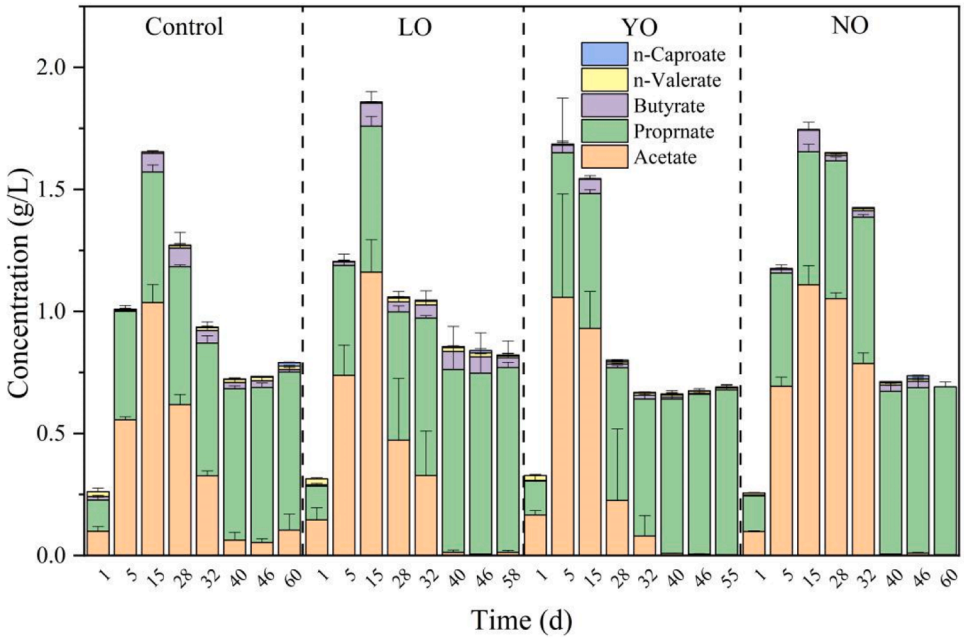

Fig. 2. Changes of individual VFA in the presence of LO, YO, and NO during the AD process.

the propionate degradation was inhibited, indicating that the syntrophic propionate-oxidizing process were severely inhibited under high ammonia conditions (Guo et al., 2024). *Trichococcus* has been reported as a putative electroactive bacterium that can utilize acetate and perform the EET process (Ma et al., 2021; Ren et al., 2020), suggesting that REOs contributed to the enrichment of ammonia-tolerant electroactive microbes and the enhancement of acetate degradation.

As shown in Fig. 4b, the dominant methanogens were *Methanosaeta, Methanosarcina, Methanospirillum*, and *Methanobacterium*. The relative abundances of Methanosaeta decreased on average by 14 % in the presence of LO, YO, and NO *Methanosaeta* has ability to produce methane from via the DIET and acetate decarboxylation pathways (Ren et al., 2020; Zhao et al., 2020), implying that its role was weakened in promoting methanogenesis due to the ammonia inhibitory effect. However, when LO, YO, and NO were added into the AD systems, the relative abundances of *Methanosarcina, Methanospirillum*, and *Methanobacterium* increased on average by 190 %, 44 %, and 34 %, respectively. Previous studies reported that *Methanosarcina* can produce methane via the DIET and acetate decarboxylation pathways (Holmes et al., 2021; Zhang et al., 2022), and that *Methanospirillum* and *Methanobacterium* can produce methane through interspecies hydrogen transfer (IHT) (Chen et al., 2018; Zhou et al., 2024). Thus, it was possible that REOs enriched different functional methanogens to enhance methane production under high ammonia concentrations.

3.5. Metabolism prediction

As shown in Fig. S4, compared to the control group, the relative abundances of carbohydrate metabolism such as citrate cycle (ko00020), glycolysis/gluconeogenesis (ko00010), pentose phosphate pathway (ko00030), pyruvate metabolism (ko00620), and starch and sucrose metabolism (ko00500) in the LO group increased by 1.4 %, 3.7 %, 3.9 %, 1.1 %, and 6.9 %, respectively. Notably, the relative abundances of the aforementioned carbohydrate metabolism pathways except for ko00020 increased by an average of 10.4 % in the YO group. However, NO caused only a 1 % increase in the relative abundance of ko00020, while it exerted a negative effect on other carbohydrate metabolism pathways. Moreover, the relative abundances of most amino

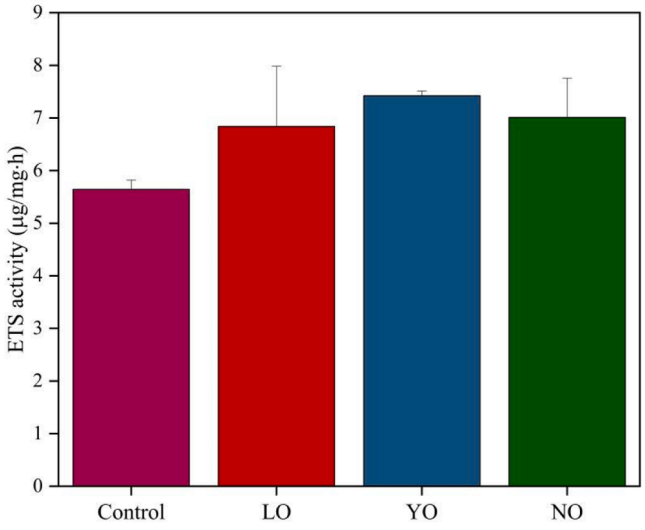

Fig. 3. Changes of ETS activity in the REO-amended AD systems.

acid metabolism pathways decreased on average by 11 % in the LO group. In contrast, the abundances of all such pathways declined on average by 11.8 % and 5 % in the YO and NO groups, respectively. Previous studies showed that the carbohydrate metabolisms can provide substrate for acidogenesis, and that amino acid metabolism can be converted to acetyl-CoA for subsequent methane production (Liu et al., 2025; Xu et al., 2025; Zhu et al., 2022). Thus, it was possible that LO and NO could promote methanogenesis by stimulating carbohydrate metabolism, thereby increasing the supply of intermediates for methane production. In addition, YO caused a mere 1.9 % increase in the relative abundance of propanoate metabolism (ko00640), while LO and NO had a negative effect. The relative abundances of fatty acid degradation pathway (ko00071) and butanoate metabolism (ko00650) decreased on average by 10.3 %, 11 %, and 5.6 % in the LO, YO and NO groups, respectively. These findings suggested that REOs had a limited ability to regulate the degradation of propionate, butyrate, and fatty acids under high ammonia concentrations.

Oxidative phosphorylation pathway can generate energy for maintaining life activities of microbial cells (Xu et al., 2025). The key modules of this pathway include NADH:quinone oxidoreductase (M00144), succinate dehydrogenase (M00149), cytochrome bd complex (M00153), and cytochrome c oxidase (M00155 and M00156) are the key components (Jiang et al., 2024). As shown in Fig. S5, compared to the control, LO led to an increase of up to 6.7 % in the gene abundances of M00153 and a decrease in the abundances of most genes in the other modules. YO caused an increase of up to 34.4 % in the gene abundances of M00155 and M00156 and a decrease in the abundances of all genes in the other modules. NO resulted in a decrease of up to 8.8 % in the gene abundances of M00153 and an increase in the abundances of partial genes in the other modules. These findings suggested that the impact of REOs on the oxidative phosphorylation pathway was type-specific. Moreover, the oxidative phosphorylation pathway can establish an electrochemical gradient, which is then utilized by bacterial F-type ATPases (M00157) and archaeal V/A-type ATPases (M00159) to drive ATP synthesis (Zhao et al., 2020). As shown in Fig. S6, in comparison to the control group, the relative abundances of most genes in M00157 and M00159 increased on average by 1.7 % and 1.9 % in the LO group, respectively, while YO exhibited only a positive effect on M00157. However, as for the NO group, a widespread decrease was observed in the abundance of genes in M00157 and M00159. These findings suggested that LO could effectively stimulate ATP synthesis in both bacterial and archaeal communities compared to YO and NO.

As illustrated in Fig. S7, the relative abundances of genes encoding key enzymes in methanol (M00356) and (Di/Tri) methylamine (M00563) pathways showed considerable increases (up to 2.4-fold) in the presence of REOs, particularly for NO In addition, LO, YO, and NO caused clear increases in the relative abundances of most genes encoding key enzymes in the acetate decarboxylation pathway (M00357). Moreover, as for the carbon dioxide reduction (M00567), previous reports showed that the genes (e.g., *fwdA-E* and *mtd*) were related to the DIET-based CO_2-dependent methanogenesis (Zhao et al., 2020; Zhu et al., 2022). However, only the relative abundances of *fwdA and fwdB* showed an increase in the presence of LO, YO and NO, suggesting that the regulatory effect of REOs on the DIET-based methane metabolism was weakened. Notably, REOs caused increases (up to 48.5 %) in the relative abundances of *fwdH, fwdF* and *mch*, suggesting that the IHT-driven methanogenic pathway might make important contribution to methanogenesis (Dai et al., 2024). Overall, these findings potentially indicated that REOs could stimulate multiple methanogenic pathways to enhance methanogenesis under high ammonia concentrations.

3.6. Role of REOs in methanogenesis

This work demonstrated that the stimulatory effects of REOs on methanogenesis were highly dependent on their types under high ammonia concentrations. Specifically, LO and YO can effectively improve methane yield and Rm, while NO had the ability to improve methane yield rather than Rm. In addition, the addition of LO, YO and NO altered the microbial community composition and enriched different

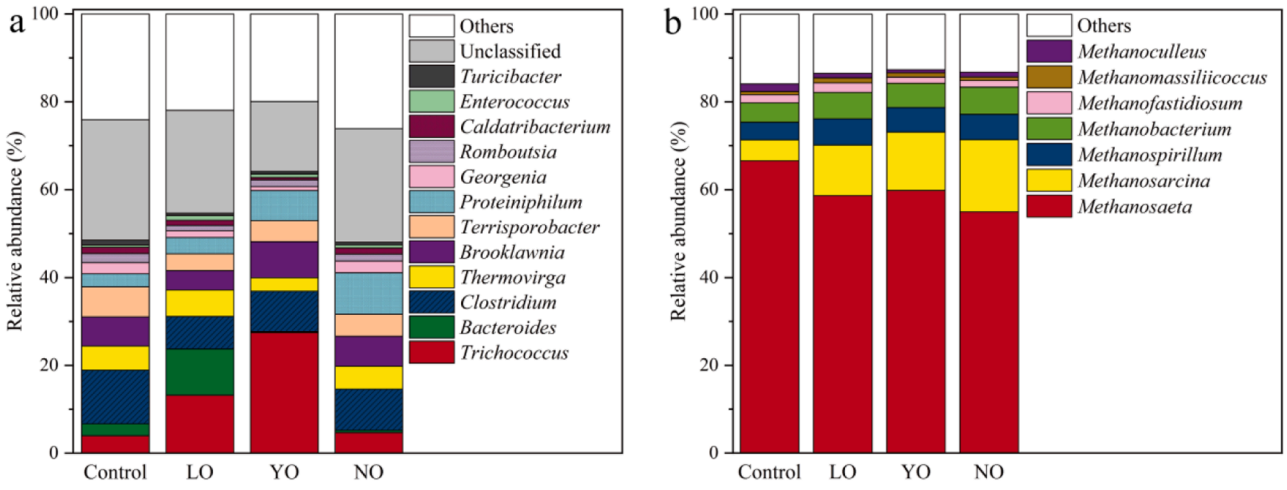

Fig. 4. The relative abundance of bacterial (a) and archaeal (b) communities at the level of genus.

types of acidogenic bacteria and methanogens, concomitant with the change in the electrochemical response pattern and the varied compositions and concentrations of VFAs during AD. Notably, the REO addition facilitated the degradation of acetate rather than propionate. The over-accumulation of propionate was observed in the presence of REOs. It was possible that the activity of propionate-oxidating bacteria could be seriously inhibited under high ammonia stress, thereby disrupting their syntrophic cooperation with methanogens (Bonk et al., 2018; Guo et al., 2024; Lee et al., 2019; Yang et al., 2024). In this work, REOs could have a low regulating ability to improve propionate metabolism (Fig. S4), which resulted in a low syntrophic conversion of propionate to methane.

It has been reported that *Trichococcus* was a putative electroactive bacterium that can utilize acetate and establish DIET with methanogens such as *Methanosaeta* (Ma et al., 2021; Ren et al., 2020). *Methanosarcina* has been reported to have the ability to accept exogenous electron to drive the conversion of CO_2 to methane via the conductive materials (Holmes et al., 2021; Liu et al., 2025). In this work, LO caused an enrichment of *Trichococcus* and *Methanosarcina*. Thus, it was possible that DIET might be established between *Trichococcus* and *Methanosarcina*, thereby promoting a rapid syntrophic conversion of acetate to methane. In this process, LO could function as electron conduits to facilitate DIET due to its high EEC and the enhancement of ETS activity and electron change capability of the AD system. In addition, although the relative abundance of *Methanosaeta* decreased by 12 %, its high percentage (58.7 %) indicated its potential role in the DIET-based methanogenesis. However, apart from potentially enhancing the DIET-based syntrophic acetate metabolism, LO might also stimulate methane production via multiple pathways, including IHT and the utilization of methanol, methylamine and acetate. This is potentially supported by the increase in the relative abundances of these pathways based on the metabolic prediction (Fig. S7). Thus, LO may alleviate the ammonia inhibitory effect and enhance methanogenesis by stimulating multiple methanogenic pathways.

Prior reports showed the DIET efficiency was closely related to Rm (Lee et al., 2019; Liu et al., 2025; Xu et al., 2025). Although YO caused an enrichment of *Trichococcus* and *Methanosarcina* and enhanced the ETS activity, it did not enhance the electron exchange capacity of the AD system. In addition, Rm in the YO group declined by 5.1 % compared to the LO group, indicating the LO-mediated DIET could make a minor contribution to improving methanogenesis. Thus, the findings, combined the potential enhancement of M00356, M00563, M00357, and M00567 based on the metabolic prediction (Fig. S7), suggested that the positive effect of YO in AD mainly by potentially stimulating the other pathways such as the acetate decarboxylation and the utilization of H_2, methanol, and methylamine during the AD of DPB (Liu et al., 2018; Xiao et al., 2019). Moreover, compared to the control group, the stimulatory effect of NO was limited to methane yield and did not extend to Rm (Table S2). The possible reasons were mainly due to the facts: (1) the ETS activity and electron exchange capacity were higher in the NO group than those in the control, indicating that the microbial electron transfer capacity might be enhanced (Zhuo et al., 2025). In addition, the metabolism prediction suggested that NO could enhance the relative abundances of partial genes associated with the oxidative phosphorylation pathway. Thus, the low Rm suggested that a portion of electrons and energy could be used for supporting microbial growth (Liu et al., 2025); (2) compared to the LO and YO groups, the NO group showed a low enrichment of *Trichococcus*. The findings, combined with low EEC of NO, suggested that the stimulatory effect of NO on the putative DIET-based methanogenesis could contribute marginally to the enhanced methane production. However, the metabolism prediction showed that the relative abundances of most genes for the methanogenic pathways such as the acetate decarboxylation and the utilization of H_2, methanol, and methylamine were higher in the NO group than those in the LO and YO groups. Thus, it was possible that NO could promote methane yield mainly by stimulating multiple methanogenic pathways, while the putative DIET-based methanogenesis played a minor role. Prior reports showed that the IHT-mediated methanogenesis relies on the rate-limiting H_2 diffusion (Akram et al., 2024), thereby causing no improvement on Rm in the LO group.

Although REOs facilitated methane production from DPB under high ammonia concentrations, the methane yield obtained in this work (31 mL/g-VS) was markedly lower than the reported values for untreated DPB (85–104 mL/g-VS) (Xing et al., 2022; Xu et al., 2025). This indicated that the methanogenic activity was severely inhibited in this work. Moreover, it has been reported that the methane yield of DPB reached 181 mL/g-VS after NaOH pretreatment (Xing et al., 2022). However, this value was still lower than the reported values from other grass biomass such as *Arundo donax* L (228–266 mL/g-VS), *Pennisetum giganteum* (224.3–294.7 mL/g-VS), herbaceous garden plants (332.7 mL/g-VS), and energy crops (400–475 mL/g-VS) (Córdoba et al., 2026; Liu et al., 2025; Triolo et al., 2012). The low methane yield could be attributed to the high lignin content in DPB, due to its recalcitrance to anaerobic microbial degradation (Xing et al., 2022). Thus, future research should prioritize the development of high-performance pretreatment methods to enhance DPB biodegradability (Xue et al., 2020). Moreover, the over-accumulation of propionate, caused by ammonia inhibition, was also a key factor contributing to a low methane yield from DPB. Studies have demonstrated that bioaugmentation by adding specific microbial strains or consortia is the most effective approach to mitigating ammonia inhibition and enhancing the methanogenic performance (Li et al., 2023a). Thus, bioaugmentation with well-constructed propionate-degrading microbial strains or consortia could be beneficial for improving methane production from DPB. Overall, to address the inherent biodegradability limitations of DPB and the over-accumulation of propionate under high ammonia stress, the combination of REO amendment with DPB pretreatment and bioaugmentation is highly recommended.

4. Conclusion

This work demonstrated that the positive effects of REOs on methanogenesis were highly dependent on their types under high ammonia concentrations. LO and YO can effectively improve methane yield and Rm, while NO had the ability to improve methane yield rather than Rm. LO, YO, and NO altered the microbial community composition, causing a selective enrichment of different types of the acidogenic bacteria and methanogens and changes in the electrochemical response pattern of the AD systems. Apart from stimulating the putative DIET-based syntrophic acetate metabolism between *Trichococcus* and *Methanosarcina*, LO could also facilitate methanogenesis, potentially by enhancing alternative pathways such as IHT, utilization of methanol and methylamine, and acetate decarboxylation. Moreover, YO and NO promoted methane yield likely by enhancing the acetate decarboxylation and the utilization of H_2, methanol, and methylamine, whereas putative DIET-based methanogenesis played only a minor role. Overall, REOs could alleviate the ammonia inhibitory effect and enhance methanogenesis by stimulating multiple methanogenic pathways. This work offers practical guidance for using REOs to tackle ammonia inhibition issues and improve methanogenic performance in laboratory-scale AD systems operated in batch mode.

CRediT authorship contribution statement

Ting-ting Yang: Investigation, Formal analysis. **Zhi-Man Yang:** Writing – review & editing, Funding acquisition. **Zhi-Biao Chen:** Conceptualization. **Zu-Liang Chen:** Project administration.

Declaration of competing interest

The authors declare that they have no known competing financial interests or personal relationships that could have appeared to influence

the work reported in this paper.

Acknowledgement

This work was funded by the Program of Innovation Team Cultivation (Y0720409B06), the Award Program for Min River Scholar in Fujian Province (No. Min [2022]4), and the Natural Science Foundation of Fujian province (No. 2022J01648).

Supplementary materials

Supplementary material associated with this article can be found, in the online version, at doi:10.1016/j.teengi.2026.100070.

Data availability

Data will be made available on request.

References

Akram, J., Song, C., El Mashad, H.M., Chen, C., Zhang, R., Liu, G., 2024. Advances in microbial community, mechanisms and stimulation effects of direct interspecies electron transfer in anaerobic digestion. Biotechnol. Adv. 76, 108398. https://doi.org/10.1016/j.biotechadv.2024.108398.

Al Hasani, Z., Nayak, J.K., Al Balushi, N.J., Al-Mamun, A., Samal, K., 2025. Prospect of conductive materials in the anaerobic digester matrix for methane production: electron transfer and microbial communication. Water 17 (9), 321. https://doi.org/10.3390/w17091321.

Alhassan, S., Alshammari, K., Alshammari, M., Alotaibi, T., Alshammari, A.H., Alhamazani, A., Henini, M., Abdel Mohaymen Taha, T., 2024. Linear and nonlinear optical investigations of polyvinyl chloride modified La_2O_3 nanocomposite films. Results Phys. 58, 107456. https://doi.org/10.1016/j.rinp.2024.107456.

Baek, G., Kim, J., Kim, J., Lee, C., 2018. Role and potential of direct interspecies electron transfer in anaerobic digestion. Energies 11 (1), 107. https://doi.org/10.3390/en11010107.

Bonk, F., Popp, D., Weinrich, S., Strauber, H., Kleinsteuber, S., Harms, H., Centler, F., 2018. Ammonia inhibition of anaerobic volatile fatty acid degrading microbial communities. Front. Microbiol. 9, 2921. https://doi.org/10.3389/fmicb.2018.02921.

Cai, C., Li, L., Hua, Y., Liu, H., Dai, X., 2021a. Ferroferric oxide promotes metabolism in *anaerolineae* other than microbial syntrophy in anaerobic methanogenesis of antibiotic fermentation residue. Sci. Total Environ. 758, 143601. https://doi.org/10.1016/j.scitotenv.2020.143601.

Cai, Y., Zheng, Z., Wang, X., 2021b. Obstacles faced by methanogenic archaea originating from substrate-driven toxicants in anaerobic digestion. J. Hazard. Mater. 403, 123938. https://doi.org/10.1016/j.jhazmat.2020.123938.

Chen, G., Li, Y., Qi, W., Yang, C., Zhao, X., 2017. Morphology-tailored synthesis and luminescent properties of Y_2O_3: eu^{3+} phosphors. J. Mater. Sci.: Mater. Electron. 29 (4), 2841–2847. https://doi.org/10.1007/s10854-017-8213-7.

Chen, S., He, J., Wang, H., Dong, B., Li, N., Dai, X., 2018. Microbial responses and metabolic pathways reveal the recovery mechanism of an anaerobic digestion system subjected to progressive inhibition by ammonia. Chem. Eng. J. 350, 312–323. https://doi.org/10.1016/j.cej.2018.05.168.

Chen, Y., Cheng, J.J., Creamer, K.S., 2008. Inhibition of anaerobic digestion process: a review. Bioresour. Technol. 99 (10), 4044–4064. https://doi.org/10.1016/j.biortech.2007.01.057.

Córdoba, V., Rodríguez, D., Manzur, A., Lázaro, L., 2026. Impact of harvest timing and ensiling on methane yield of Arundo donax L. Biomass Bioenergy 208, 108824. https://doi.org/10.1016/j.biortech.2012.08.079.

Cruz, V.C., Simonetti, S., Palma, E., Pagliaccia, P., Braguglia, C., Fazi, S., Baronti, S., Navarra, M.A., Pettiti, I., Koch, C., Harnisch, F., Aulenta, F., 2017. Enhancing methane production from food waste fermentation using biochar: the added value of electrochemical testing in pre-selecting the most effective type of biochar. Biotechnol. Biofuels 10, 303. https://doi.org/10.1186/s13068-017-0994-7.

Dai, X.F., Bai, Y., Lian, S.J., Qi, X.J., Feng, K., Fu, S.F., Guo, R.B., 2024. Distinct mechanisms between free iron species and magnetite addition in anaerobic digestion on alleviating ammonia inhibition. ACS EST Eng. 4 (8), 1990–2001. https://doi.org/10.1021/acsestengg.4c00171.

Feng, L., Chen, Z., Wang, H., Chen, Z., Chen, Z., Liu, J., Zeng, Y., 2025. A study of rare earth elements enriched carbonisation material prepared from *Dicranopteris pedata* biomass grown in mining area. Sci. Rep. 15 (1), 6486. https://doi.org/10.1038/s41598-025-86067-y.

Guo, M., Wei, S., Guo, M., Li, M., Qi, X., Wang, Y., Jia, X., 2024. Potential mechanisms of propionate degradation and methanogenesis in anaerobic digestion coupled with microbial electrolysis cell system: importance of biocathode. Bioresour. Technol. 400, 130695. https://doi.org/10.1016/j.biortech.2024.130695.

Holmes, D.E., Zhou, J., Ueki, T., Woodard, T., Lovley, D.R., 2021. Mechanisms for electron uptake by *Methanosarcina acetivorans* during direct interspecies electron transfer. mBio 12 (5), 10. https://doi.org/10.1128/mbio.02344-21.

Jiang, X., Li, Z., Lin, K., Zhao, Y., Su, L., Wu, T., Zhou, T., 2024. Enhancement of anaerobic digestion from food waste via inert substances based on metagenomic analysis: oxidative phosphorylation and metabolism. Environ. Res. 246, 118033. https://doi.org/10.1016/j.envres.2023.118033.

Kaya, E.E., Gürmen, S., 2020. A straightforward approach for the synthesis of nanostructured Y_2O_3 particles: synthesis, morphology, microstructure and crystal imperfection. Physica E. 115, 113668. https://doi.org/10.1016/j.physe.2019.113668.

Lee, J., Koo, T., Yulisa, A., Hwang, S., 2019. Magnetite as an enhancer in methanogenic degradation of volatile fatty acids under ammonia-stressed condition. J. Environ. Manag. 241, 418–426. https://doi.org/10.1016/j.jenvman.2019.04.038.

Li, J., Yao, Y., Shi, Y., Tang, J., Gadow, S.I., Liu, R., Niu, Q., 2022. Bmim]FeCl(4) mediated inhibition and toxicity during anaerobic digestion: dose-response kinetics, biochar-dependent detoxification and microbial resistance. Water Res. 210, 117969. https://doi.org/10.1016/j.watres.2021.117969.

Li, L., Liu, C., Xu, L., Zhuang, H., He, J., He, Q., Zhang, J., 2023b. Acclimation of anaerobic fermentation microbiome with acetate and ethanol for chain elongation and the biochemical response. Chemosphere 320, 138083. https://doi.org/10.1016/j.chemosphere.2023.138083.

Li, Z.Y., Inoue, D., Ike, M., 2023a. Mitigating ammonia-inhibition in anaerobic digestion by bioaugmentation: a review. J. Water Proc. Eng. 52, 103506. https://doi.org/10.1016/j.jwpe.2023.103506.

Liu, D., Roca-Puigros, M., Geppert, F., Caizan-Juanarena, L., Na Ayudthaya, S.P., Buisman, C., Ter Heijne, A., 2018. Granular carbon-based electrodes as cathodes in methane-producing bioelectrochemical systems. Front. Bioeng. Biotechnol. 6, 78. https://doi.org/10.3389/fbioe.2018.00078.

Liu, Q.H., Qiu, Y.H., Yang, Z.M., 2025. KOH activation increased biochar's capacity to regulate electron transfer and promote methanogenesis. Energy 322, 135650. https://doi.org/10.1016/j.energy.2025.135650.

Liu, Y., Ye, X., Xiao, Q., Wang, C., Jia, Z., Cao, C., Du, J., Kong, X., Xi, Y., 2022. Targeted addition of CeO_2 nanoparticles to promote methane production in anaerobic digestion systems of wheat straw. J. Clean. Prod. 377, 134231. https://doi.org/10.1016/j.jclepro.2022.134231.

Lu, D., Zhang, Q., Wang, F., Wang, H., Liu, H., Yi, W., Zhang, Z., Zhang, D., 2022. Effect of nano-Fe_3O_4 biochar on anaerobic digestion of chicken manure under high ammonia nitrogen concentration. J. Clean. Prod. 375, 134107. https://doi.org/10.1016/j.jclepro.2022.134107.

Luo, X., Xu, L., Yang, L., Zhao, J., Asefa, T., Qiu, R., Huang, Z., 2024. Ball Milling of La_2O_3 Tailors the crystal structure, reactive oxygen species, and free radical and non-free radical photocatalytic pathways. ACS Appl. Mater. Interfaces 16 (15), 18671–18685. https://doi.org/10.1021/acsami.3c15677.

Ma, K., Wang, W., Liu, Y., Bao, L., Cui, Y., Kang, W., Wu, Q., Xin, X., 2021. Insight into the performance and microbial community profiles of magnetite-amended anaerobic digestion: varying promotion effects at increased loads. Bioresour. Technol. 329, 124928. https://doi.org/10.1016/j.biortech.2021.124928.

Michel, C.R., Martínez-Preciado, A.H., Contreras, N.L.L., 2013. Gas sensing properties of Nd_2O_3 nanostructured microspheres. Sens. Actuators B Chem. 184, 8–14. https://doi.org/10.1016/j.snb.2013.04.044.

Mlinar, S., Weig, A.R., Freitag, R., 2022. Influence of NH_3 and NH_4^+ on anaerobic digestion and microbial population structure at increasing total ammonia nitrogen concentrations. Bioresour. Technol. 361, 127638. https://doi.org/10.1016/j.biortech.2022.127638.

Mu, Q., Wang, Y., 2011. Synthesis, characterization, shape-preserved transformation, and optical properties of $La(OH)_3$, $La_2O_2CO_3$, and La_2O_3 nanorods. J. Alloys Compd. 509 (2), 396–401. https://doi.org/10.1016/j.jallcom.2010.09.041.

Ngo, T., Khudur, L.S., Hakeem, I.G., Shah, K., Surapaneni, A., Ball, A.S., 2022. Wood biochar enhances the valorisation of the Anaerobic digestion of chicken manure. Clean Technol. 4 (2), 420–439. https://doi.org/10.3390/cleantechnol4020026.

Ngo, T., Khudur, L.S., Krohn, C., Hassan, S., Jansriphibul, K., Hakeem, I.G., Shah, K., Surapaneni, A., Ball, A.S., 2023. Wood biochar enhances methanogenesis in the anaerobic digestion of chicken manure under ammonia inhibition conditions. Heliyon 9 (11), e21100. https://doi.org/10.1016/j.heliyon.2023.e21100.

Okamoto, A., Hashimoto, K., Nealson, K.H., Nakamura, R., 2013. Rate enhancement of bacterial extracellular electron transport involves bound flavin semiquinones. Proc. Natl. Acad. Sci. U. S. A. 110 (19), 7856–7861. https://doi.org/10.1073/pnas.1220823110.

Qin, Y., Yin, X., Xu, X., Yan, X., Bi, F., Wu, W., 2020. Specific surface area and electron donating capacity determine biochar's role in methane production during anaerobic digestion. Bioresour. Technol. 303, 122919. https://doi.org/10.1016/j.biortech.2020.122919.

Ren, S., Usman, M., Tsang, D.C.W., S, O.T., Angelidaki, I., Zhu, X., Zhang, S., Luo, G., 2020. Hydrochar-facilitated anaerobic digestion: evidence for direct interspecies electron transfer mediated through surface oxygen-containing functional groups. Environ. Sci. Technol. 54 (9), 5755–5766. https://doi.org/10.1021/acs.est.0c00112.

Rotaru, A.-E., Shrestha, P.M., Liu, F., Shrestha, M., Shrestha, D., Embree, M., Zengler, K., Wardman, C., Nevin, K.P., Lovley, D.R., 2014. A new model for electron flow during anaerobic digestion: direct interspecies electron transfer to *Methanosaeta* for the reduction of carbon dioxide to methane. Energy Environ. Sci. 7 (1), 408–415. https://doi.org/10.1039/c3ee42189a.

Shapovalov, Y., Zhadan, S., Bochmann, G., Salyuk, A., Nykyforov, V., 2020. Dry anaerobic digestion of chicken manure: a review. Appl. Sci. 10 (21), 7825. https://doi.org/10.3390/app10217825.

Shi, X., Lin, J., Zuo, J., Li, P., Li, X., Guo, X., 2017. Effects of free ammonia on volatile fatty acid accumulation and process performance in the anaerobic digestion of two typical bio-wastes. J. Environ. Sci. 55, 49–57. https://doi.org/10.1016/j.jes.2016.07.006.

Shi, X., Wang, S., Wang, Z., Wu, G., Hu, Z., Zhan, X., 2024. Ammonia-induced constraints on butyrate degradation in anaerobic digestion: impact of ammonia levels and pH conditions, and recovery behaviour. Int. Biodeterior. Biodegrad. 193, 105847. https://doi.org/10.1016/j.ibiod.2024.105847.

Su, K., Li, L., Zeng, Z., Yang, X., Lei, T., Zhang, H., Wang, Q., Cao, R., 2024. The double-edged effects of La_2O_3 and CeO_2 on the performance of high-rate anaerobic sludge bed reactors and microbial mechanisms. Process Saf. Environ. Prot. 184, 377–390. https://doi.org/10.1016/j.psep.2024.01.095.

Triolo, J.M., Pedersen, L., Qu, H., Sommer, S.G., 2012. Biochemical methane potential and anaerobic biodegradability of non-herbaceous and herbaceous phytomass in biogas production. Bioresour. Technol. 125, 226–232. https://doi.org/10.1016/j.biortech.2012.08.079.

Tripathi, H., Sharma, J.D., Kumar, S., Bhardwaj, S., 2024. Effect of La_2O_3 as sintering aid on the structural, mechanical & electrical properties of Y_2O_3. Mater. Sci. Eng., B 303, 117259. https://doi.org/10.1016/j.mseb.2024.117259.

Wang, G., Fu, P., Zhang, B., Zhang, J., Huang, Q., Yao, G., Li, Q., Dzakpasu, M., Zhang, J., Li, Y.-Y., Chen, R., 2023a. Biochar facilitates methanogens evolution by enhancing extracellular electron transfer to boost anaerobic digestion of swine manure under ammonia stress. Bioresour. Technol. 388, 129773. https://doi.org/10.1016/j.biortech.2023.129773.

Wang, M., Zhao, Z., Zhang, Y., 2021. Magnetite-contained biochar derived from fenton sludge modulated electron transfer of microorganisms in anaerobic digestion. J. Hazard. Mater. 403, 123972. https://doi.org/10.1016/j.jhazmat.2020.123972.

Wang, Z.-K., Liu, Q.-H., Yang, Z.-M., 2023b. Nano magnetite-loaded biochar boosted methanogenesis through shifting microbial community composition and modulating electron transfer. Sci. Total Environ. 861, 160597. https://doi.org/10.1016/j.scitotenv.2022.160597.

Wu, Z., Nguyen, D., Lam, T.Y.C., Zhuang, H., Shrestha, S., Raskin, L., Khanal, S.K., Lee, P. H., 2021. Synergistic association between cytochrome bd-encoded *proteiniphilum* and reactive oxygen species (ROS)-scavenging methanogens in microaerobic-anaerobic digestion of lignocellulosic biomass. Water Res. 190, 116721. https://doi.org/10.1016/j.watres.2020.116721.

Xiao, B., Wang, X., He, E., Zuo, Y., Wan, L., Li, L., 2024. Effects of microbial electrolysis cell on anaerobic digestion of food waste: acidification and recovery. Fuel 369, 131756. https://doi.org/10.1016/j.fuel.2024.131756.

Xiao, L., Sun, R., Zhang, P., Zheng, S., Tan, Y., Li, J., Zhang, Y., Liu, F., 2019. Simultaneous intensification of direct acetate cleavage and CO_2 reduction to generate methane by bioaugmentation and increased electron transfer. Chem. Eng. J. 378, 122229. https://doi.org/10.1016/j.cej.2019.122229.

Xing, T., Wang, Z., Zhen, F., Liu, H., Wang, F., Zhang, Y., Kong, X., Sun, Y., 2022. Methane production of rare earth element-rich *dicranopteris dichotoma* and effects of La(III) on anaerobic digestion performance of lignocellulose. J. Chem. Technol. Biotechnol. 97 (8), 1987–1994. https://doi.org/10.1002/jctb.7068.

Xu, J., Kumar Khanal, S., Kang, Y., Zhu, J., Huang, X., Zong, Y., Pang, W., Surendra, K.C., Xie, L., 2022. Role of interspecies electron transfer stimulation in enhancing anaerobic digestion under ammonia stress: mechanisms, advances, and perspectives. Bioresour. Technol. 360, 127558. https://doi.org/10.1016/j.biortech.2022.127558.

Xu, J., Shi, Z., Xu, L., Zheng, X., Zong, Y., Luo, G., Zhang, C., Liu, M., Xie, L., 2024. Recovery capability of anaerobic digestion from ammonia stress: metabolic activity, energy generation, and genome-centric metagenomics. Bioresour. Technol. 394, 130203. https://doi.org/10.1016/j.biortech.2023.130203.

Xu, K.X., Qiu, Y.H., Chen, Z.B., Chen, Z.L., Xiu, P., Yang, Z.M., 2025. Deciphering the role and mechanism of rare earth element-rich biochar during anaerobic digestion of *Dicranopteris pedata* biomass. Fuel 381, 133720. https://doi.org/10.1016/j.fuel.2024.133720.

Xue, Y., Li, Q., Gu, Y., Yu, H., Zhang, Y., Zhou, X., 2020. Improving biodegradability and biogas production of miscanthus using a combination of hydrothermal and alkaline pretreatment. Ind. Crop. Prod. 144, 111985. https://doi.org/10.1016/j.indcrop.2019.111985.

Yan, P., Zhao, Y., Zhang, H., Chen, S., Zhu, W., Yuan, X., Cui, Z., 2020. A comparison and evaluation of the effects of biochar on the anaerobic digestion of excess and anaerobic sludge. Sci. Total Environ. 736, 139159. https://doi.org/10.1016/j.scitotenv.2020.139159.

Yang, J., Zhang, J., Du, X., Gao, T., Cheng, Z., Fu, W., Wang, S., 2024. Ammonia inhibition in anaerobic digestion of organic waste: a review. Int. J. Environ. Sci. Technol. 22 (5), 3927–3942. https://doi.org/10.1007/s13762-024-06029-1.

Yang, Z.M., Guo, R.B., Dong, X.H., 2022. Promoting biomethane production from propionate with Fe_2O_3@carbon nanotubes composites. Sci. Total Environ. 818, 151762. https://doi.org/10.1016/j.scitotenv.2021.151762.

Yin, Q., Gu, M., Wu, G., 2020. Inhibition mitigation of methanogenesis processes by conductive materials: a critical review. Bioresour. Technol. 317, 123977. https://doi.org/10.1016/j.biortech.2020.123977.

Zhang, M., Guo, H., Xia, D., Dong, Z., Liu, X., Zhao, W., Jia, J., Yin, X., 2022. Metagenomic insight of corn straw conditioning on substrates metabolism during coal anaerobic fermentation. Sci. Total Environ. 808, 152220. https://doi.org/10.1016/j.scitotenv.2021.152220.

Zhao, Z., Wang, J., Li, Y., Zhu, T., Yu, Q., Wang, T., Liang, S., Zhang, Y., 2020. Why do DIETers like drinking: metagenomic analysis for methane and energy metabolism during anaerobic digestion with ethanol. Water Res. 171, 115425. https://doi.org/10.1016/j.watres.2019.115425.

Zhou, L., Lu, B., Mo, L., Du, L., Pan, S., Wei, Y., 2024. Ethanol-coupled bioelectrochemical anaerobic digestion system promotes electron mutualistic of electroactive bacteria to enhance propionate degradation and methanogenesis. Fuel 373, 132387. https://doi.org/10.1016/j.fuel.2024.132387.

Zhu, L., Wu, B., Liu, Y., Zhang, J., Deng, R., Gu, L., 2022. Strategy to enhance semi-continuous anaerobic digestion of food waste by combined use of calcium peroxide and magnetite. Water Res. 221, 118801. https://doi.org/10.1016/j.watres.2022.118801.

Zhuo, Y., Wang, H., Wang, X., Jing, D., Zhou, M., Peng, D., Han, Y., 2025. Performance of electroactive anaerobic granular sludge under ammonia stress: performance, microbe and morphology. Bioresour. Technol. 424, 132295. https://doi.org/10.1016/j.biortech.2025.132295.